

World Journal of *Diabetes*

World J Diabetes 2024 July 15; 15(7): 1384-1653



EDITORIAL

- 1384 Remission of type 2 diabetes mellitus
Nakhleh A, Halfin E, Shehadeh N
- 1390 Diabetes remission and nonalcoholic fatty pancreas disease
Wu WJ
- 1394 Management of gestational diabetes mellitus *via* nutritional interventions: The relevance of gastric emptying
Huang WK, Jalleh RJ, Rayner CK, Wu TZ
- 1398 MicroRNA-630: A promising avenue for alleviating inflammation in diabetic kidney disease
Donate-Correa J, González-Luis A, Díaz-Vera J, Hernandez-Fernaud JR
- 1404 Adiposity in Chinese people with type 1 diabetes
Wu NW, Lyu XF, An ZM, Li SY
- 1409 Diabetes and tuberculosis: An emerging dual threat to healthcare
Shetty S, Pappachan JM, Fernandez CJ

REVIEW

- 1417 Patient-centered care in diabetes care-concepts, relationships and practice
Chen TT, Su WC, Liu MI
- 1430 Insulin resistance as the molecular link between diabetes and Alzheimer's disease
Abdalla MMI

MINIREVIEWS

- 1448 Obstructive sleep apnea: Overlooked comorbidity in patients with diabetes
Tenda ED, Henrina J, Cha JH, Triono MR, Putri EA, Aristy DJ, Tahapary DL
- 1461 Update on evidence-based clinical application of sodium-glucose cotransporter inhibitors: Insight to uncommon cardiovascular disease scenarios in diabetes
Tao SB, Lu X, Ye ZW, Tong NW

ORIGINAL ARTICLE**Retrospective Cohort Study**

- 1477 Association between glucose levels of children with type 1 diabetes and parental economic status in mobile health application

Zhang WH, Wang CF, Wang H, Tang J, Zhang HQ, Zhu JY, Zheng XY, Luo SH, Ding Y

Retrospective Study

- 1489 Association between glucose-lowering drugs and circulating insulin antibodies induced by insulin therapy in patients with type 2 diabetes

Zhang P, Jiang Q, Ding B, Yan RN, Hu Y, Ma JH

- 1499 Clinical efficacy of endovascular revascularization combined with vacuum-assisted closure for the treatment of diabetic foot

Lei FR, Shen XF, Zhang C, Li XQ, Zhuang H, Sang HF

- 1509 Magnetic resonance imaging combined with serum endolipin and galactaglobin-3 to diagnose cerebral infarction in the elderly with diabetes mellitus

Zhang YH, Liang D

- 1518 Dapagliflozin in heart failure and type 2 diabetes: Efficacy, cardiac and renal effects, safety

Yu PL, Yu Y, Li S, Mu BC, Nan MH, Pang M

Observational Study

- 1531 Cut-off value of glycated hemoglobin A1c for detecting diabetic retinopathy in the Chinese population

Wen Y, Wang Q

- 1537 Glymphatic function and its influencing factors in different glucose metabolism states

Tian B, Zhao C, Liang JL, Zhang HT, Xu YF, Zheng HL, Zhou J, Gong JN, Lu ST, Zeng ZS

Clinical and Translational Research

- 1551 Does type 1 diabetes serve as a protective factor against inflammatory bowel disease: A Mendelian randomization study

Tong KK, Yu YF, Yang XY, Wu JY, Yu R, Tan CC

- 1562 Network pharmacology and molecular dynamics study of the effect of the *Astragalus-Coptis* drug pair on diabetic kidney disease

Zhang MY, Zheng SQ

Basic Study

- 1589 Interactions between myoblasts and macrophages under high glucose milieu result in inflammatory response and impaired insulin sensitivity

Luo W, Zhou Y, Wang LY, Ai L

SYSTEMATIC REVIEWS

- 1603** Natural product-based treatment potential for type 2 diabetes mellitus and cardiovascular disease
Shrivastav D, Kumbhakar SK, Srivastava S, Singh DD

META-ANALYSIS

- 1615** Evaluation of teplizumab's efficacy and safety in treatment of type 1 diabetes mellitus: A systematic review and meta-analysis
Ma XL, Ge D, Hu XJ

SCIENTOMETRICS

- 1627** Global trends in publications regarding macrophages-related diabetic foot ulcers in the last two decades
Wen JP, Ou SJ, Liu JB, Zhang W, Qu YD, Li JX, Xia CL, Yang Y, Qi Y, Xu CP

LETTER TO THE EDITOR

- 1645** Atrial fibrillation and prediabetes: A liaison that merits attention!
Batta A, Hatwal J
- 1648** Serum tumor markers: Can they clinically implicate in type 2 diabetes mellitus?
Reddy KS, Pandiaraj IP, Gaur A, Varatharajan S
- 1651** Bidirectional link between periodontitis and systemic inflammation in diabetic retinopathy
Nishant P, Sinha S, Sinha RK, Morya AK

ABOUT COVER

Peer Review of *World Journal of Diabetes*, Erkan Gokce, MD, Professor, Department of Radiology, Tokat Gaziosmanpasa University, School of Medicine, Tokat 60100, Türkiye. drerkangokce@gmail.com

AIMS AND SCOPE

The primary aim of *World Journal of Diabetes* (*WJD*, *World J Diabetes*) is to provide scholars and readers from various fields of diabetes with a platform to publish high-quality basic and clinical research articles and communicate their research findings online.

WJD mainly publishes articles reporting research results and findings obtained in the field of diabetes and covering a wide range of topics including risk factors for diabetes, diabetes complications, experimental diabetes mellitus, type 1 diabetes mellitus, type 2 diabetes mellitus, gestational diabetes, diabetic angiopathies, diabetic cardiomyopathies, diabetic coma, diabetic ketoacidosis, diabetic nephropathies, diabetic neuropathies, Donohue syndrome, fetal macrosomia, and prediabetic state.

INDEXING/ABSTRACTING

The *WJD* is now abstracted and indexed in Science Citation Index Expanded (SCIE, also known as SciSearch®), Current Contents/Clinical Medicine, Journal Citation Reports/Science Edition, PubMed, PubMed Central, Reference Citation Analysis, China Science and Technology Journal Database, and Superstar Journals Database. The 2024 Edition of Journal Citation Reports® cites the 2023 journal impact factor (JIF) for *WJD* as 4.2; JIF without journal self cites: 4.1; 5-year JIF: 4.2; JIF Rank: 40/186 in endocrinology and metabolism; JIF Quartile: Q1; and 5-year JIF Quartile: Q2.

RESPONSIBLE EDITORS FOR THIS ISSUE

Production Editor: *Yu-Xi Chen*; Production Department Director: *Xu Guo*; Cover Editor: *Jia-Ru Fan*.

NAME OF JOURNAL

World Journal of Diabetes

ISSN

ISSN 1948-9358 (online)

LAUNCH DATE

June 15, 2010

FREQUENCY

Monthly

EDITORS-IN-CHIEF

Lu Cai, Md. Shahidul Islam, Michael Horowitz

EDITORIAL BOARD MEMBERS

<https://www.wjgnet.com/1948-9358/editorialboard.htm>

PUBLICATION DATE

July 15, 2024

COPYRIGHT

© 2024 Baishideng Publishing Group Inc

INSTRUCTIONS TO AUTHORS

<https://www.wjgnet.com/bpg/gerinfo/204>

GUIDELINES FOR ETHICS DOCUMENTS

<https://www.wjgnet.com/bpg/GerInfo/287>

GUIDELINES FOR NON-NATIVE SPEAKERS OF ENGLISH

<https://www.wjgnet.com/bpg/gerinfo/240>

PUBLICATION ETHICS

<https://www.wjgnet.com/bpg/GerInfo/288>

PUBLICATION MISCONDUCT

<https://www.wjgnet.com/bpg/gerinfo/208>

ARTICLE PROCESSING CHARGE

<https://www.wjgnet.com/bpg/gerinfo/242>

STEPS FOR SUBMITTING MANUSCRIPTS

<https://www.wjgnet.com/bpg/GerInfo/239>

ONLINE SUBMISSION

<https://www.f6publishing.com>

Basic Study

Interactions between myoblasts and macrophages under high glucose milieus result in inflammatory response and impaired insulin sensitivity

Wei Luo, Yue Zhou, Li-Ying Wang, Lei Ai

Specialty type: Endocrinology and metabolism**Provenance and peer review:** Unsolicited article; Externally peer reviewed.**Peer-review model:** Single blind**Peer-review report's classification****Scientific Quality:** Grade B, Grade C, Grade C**Novelty:** Grade C**Creativity or Innovation:** Grade C**Scientific Significance:** Grade C**P-Reviewer:** de Melo FF, Brazil**Received:** February 22, 2024**Revised:** April 28, 2024**Accepted:** May 20, 2024**Published online:** July 15, 2024**Processing time:** 136 Days and 17.6 Hours**Wei Luo**, Department of Sports and Health Sciences, Nanjing Sport Institute, Nanjing 210014, Jiangsu Province, China**Yue Zhou, Li-Ying Wang**, Department of Exercise Physiology, Beijing Sport University, Beijing 100084, China**Lei Ai**, Department of Sports Physiology Research, Jiangsu Research Institute of Sports Science, Nanjing 210033, Jiangsu Province, China**Corresponding author:** Lei Ai, PhD, Associate Research Scientist, Department of Sports Physiology Research, Jiangsu Research Institute of Sports Science, No. 169 Xianlin Avenue, Nanjing 210033, Jiangsu Province, China. ailei_982@163.com

Abstract

BACKGROUND

Skeletal muscle handles about 80% of insulin-stimulated glucose uptake and become the major organ occurring insulin resistance (IR). Many studies have confirmed the interactions between macrophages and skeletal muscle regulated the inflammation and regeneration of skeletal muscle. However, despite of the decades of research, whether macrophages infiltration and polarization in skeletal muscle under high glucose (HG) milieus results in the development of IR is yet to be elucidated. C2C12 myoblasts are well-established and excellent model to study myogenic regulation and its responses to stimulation. Further exploration of macrophages' role in myoblasts IR and the dynamics of their infiltration and polarization is warranted.

AIM

To evaluate interactions between myoblasts and macrophages under HG, and its effects on inflammation and IR in skeletal muscle.

METHODS

We detected the polarization status of macrophages infiltrated to skeletal muscles of IR mice by hematoxylin and eosin and immunohistochemical staining. Then, we developed an *in vitro* co-culture system to study the interactions between myoblasts and macrophages under HG milieus. The effects of myoblasts on macrophages were explored through morphological observation, CCK-8 assay,

Flow Cytometry, and enzyme-linked immunosorbent assay. The mediation of macrophages to myogenesis and insulin sensitivity were detected by morphological observation, CCK-8 assay, Immunofluorescence, and 2-NBDG assay.

RESULTS

The F4/80 and co-localization of F4/80 and CD86 increased, and the myofiber size decreased in IR group ($P < 0.01$, $g = 6.26$). Compared to Mc group, F4/80+CD86+CD206- cells, tumor necrosis factor- α (TNF α), interleukin-1 β (IL-1 β) and IL-6 decreased, and IL-10 increased in McM group ($P < 0.01$, $g > 0.8$). In McM + HG group, F4/80+CD86+CD206- cells, monocyte chemoattractant protein 1, TNF α , IL-1 β and IL-6 were increased, and F4/80+CD206+CD86- cells and IL-10 were decreased compared with Mc + HG group and McM group ($P < 0.01$, $g > 0.8$). Compared to M group, myotube area, myotube number and E-MHC were increased in MMc group ($P < 0.01$, $g > 0.8$). In MMc + HG group, myotube area, myotube number, E-MHC, GLUT4 and glucose uptake were decreased compared with M + HG group and MMc group ($P < 0.01$, $g > 0.8$).

CONCLUSION

Interactions between myoblasts and macrophages under HG milieu results in inflammation and IR, which support that the macrophage may serve as a promising therapeutic target for skeletal muscle atrophy and IR.

Key Words: Macrophages phenotype; Myoblasts; Cross-talk; Glucose toxicity; Chronic inflammation; Insulin sensitivity

©The Author(s) 2024. Published by Baishideng Publishing Group Inc. All rights reserved.

Core Tip: This study demonstrated interactions between myoblasts and macrophages under high glucose (HG) milieu induced pro-inflammatory M1 polarization of macrophages to exacerbate inflammatory response. Subsequently, chronic inflammation induced by HG-related M1 macrophages damaged myogenesis and insulin sensitivity in myoblasts. Ultimately, interactions between myoblasts and macrophages resulted in skeletal muscle insulin resistance (IR), which supported macrophage may serve as a promising therapeutic target for skeletal muscle atrophy and IR. This is the first research about the mediation of macrophages to HG-related myogenic inhibition and IR in myoblasts, which provide new insights into the prevention and treatment of skeletal muscle atrophy and IR.

Citation: Luo W, Zhou Y, Wang LY, Ai L. Interactions between myoblasts and macrophages under high glucose milieu result in inflammatory response and impaired insulin sensitivity. *World J Diabetes* 2024; 15(7): 1589-1602

URL: <https://www.wjgnet.com/1948-9358/full/v15/i7/1589.htm>

DOI: <https://dx.doi.org/10.4239/wjd.v15.i7.1589>

INTRODUCTION

The prevalence of diabetes, especially type 2 diabetes mellitus (T2DM), has been dramatically increasing in China, from 10.9% in 2013 to 12.4% in 2018. Insulin resistance (IR) is considered as the pathogenic driver of T2DM and precedes non-physiologic elevated plasma glucose levels, which is the primary clinical symptom of T2DM. In the prediabetic condition, insulin levels increase to meet normal insulin requirements leading to chronic hyperinsulinemia, hyperglycemia-induced β -cell failure, and eventually leads to T2DM[1,2]. The IR is defined physiologically as a state of reduced responsiveness in insulin-targeting tissues to high physiological insulin levels[3], which essentially reduced the insulin-activated glucose transport and metabolism in its target organs[4]. Skeletal muscle is one of the most important target organs of insulin, which handles about 80% of insulin-stimulated glucose uptake[5,6]. Numerous research have demonstrated the vicious cycle between myoatrophy and IR in skeletal muscle that promotes the further development of IR[7,8]. Atrophy in skeletal muscle impairs its insulin sensitivity by inhibiting glycometabolism, whereas, skeletal muscle hypertrophy and remodeling promote its insulin sensitivity[9-12]. Although the pathogenesis for IR has not yet been fully elucidated, increasing evidence prove that the chronic inflammatory response in insulin-targeting tissues plays an important role in the occurrence and development of IR[13,14].

Macrophages are one of the most abundant immunocyte populations infiltrating into tissues and can be polarized towards either pro-inflammatory M1 phenotype or anti-inflammatory M2 phenotype to regulate inflammatory responses [15,16]. The adipose tissues in obesity-induced IR subjects is characterized by the infiltration of pro-inflammatory M1 macrophages[17,18]. Meanwhile, accumulation of pro-inflammatory M1 macrophages are also reported in liver[19] and pancreatic islets[20] of IR subjects, which indicates that the macrophages may mediate the occurrence of IR. Although macrophage infiltration associated with IR has not been clearly reported in skeletal muscle, many studies have confirmed the interactions between skeletal muscle and macrophages that regulates the inflammatory reaction and regeneration in skeletal muscle[21,22]. Macrophages are indispensable for muscle remodeling and repair after injury, where they play either a promoting role for regeneration or a phagocytic role for degeneration depending on their polarized phenotype [23,24]. However, whether the interactions between skeletal muscle and macrophages results in the development of IR is

yet to be elucidated. Therefore, this study focuses on macrophages to investigate the potential mechanism behind the chronic inflammation induced IR in skeletal muscle.

Our previous research to establish IR mice model has observed that the fasting blood glucose in mice fed with high-fat diet was significantly elevated at the early stage of treatment (about 7th weeks)[25], which indicates that the high glucose (HG) milieu may be an early factor to induce IR. In line with our previous finding, a large body of data supports the HG per se can induce desensitization of insulin action to induce IR[26-28]. Whereas, effective blood glucose control can improve insulin sensitivity in skeletal muscle[29] and adipocytes[30]. HG is generally thought of as a factor that induces tissue and cell harm and dysfunction, commonly known as “glucose toxicity”[31]. However, despite of the decades of research, the pathogenesis of IR induced by HG still remains unclear. Hence, in this study, we treated macrophages and myoblasts with HG medium to explore the pathogeny of IR in skeletal muscle.

In the present study, we first detected cross-sectional area of myofiber and polarization states of macrophages in skeletal muscle of IR mice. Subsequently, to explore interactions between myoblasts and macrophages under HG milieu, we prepared a co-culture system of C2C12 myoblasts and RAW264.7 macrophages *in vitro* in the absence or presence of HG. Our results, for the first time, demonstrated the mediation of macrophages to HG-related myogenic inhibition and IR in myoblasts, which may help to understand the pathogeny of IR in skeletal muscle and the involvement of macrophages. Our study may contribute to further explore the influences of HG milieu on inflammatory response and insulin sensitivity in skeletal muscle *in vivo*.

MATERIALS AND METHODS

Animals and treatments

Male C57BL/6H mice were purchased at 5–6 wk old from Charles River Laboratories (Beijing, China). They were free fed in chamber with comfortable room temperature between 22–25 °C with 12 h day-night cycle. After one week of adaptation, animals were randomly fed with one of two diets for 12 wk: Normal standard diet (Con group, 3.42 kcal/g, 12% of energy from fat) or high-fat diet (IR group, 5.24 kcal/g, 60% of energy from fat). The contents of mineral and vitamin in these two diets was identical. This study was approved by the Institutional Animal Care and Use Committee of Nanjing Sport Institute (Protocol No. GZRDW-2022-02).

Glucose tolerance test and insulin tolerance test

Mice were fasted for 12 h and received *i.p.* injection of glucose (2 g/kg)[32,33]. The blood samples were collected from the tail vein and serum glucose level was determined at time 0, 30, 60, 90, and 120 min using glucometer (ACCU-CHEK Performa Roche, Germany). For insulin tolerance test (ITT), mice were fasted for 4 h and received *i.p.* injection of insulin (0.75 U/kg)[33-35]. The blood samples were collected and glucose concentrations were measured at time 0, 15, 30, 60, and 120 min using glucometer.

Euthanasia

After 12 wk of intervention, animals from Con and IR group ($n = 6$) were deeply anesthetized after deprived from food for 12 h (sodium amytal, *i.p.*, 150 mg/kg). The left and right gastrocnemius muscles were then removed for further biochemical and molecular analyses.

Determination of serum lipid and insulin level

After a 30 min standing of mice blood, serum samples were obtained by 3500xg centrifugation for 15 min at 4 °C. Biochemical parameters, including triglycerides (TG), total cholesterol (TC), high density lipoprotein-cholesterol, and low density lipoprotein-cholesterol (LDL-C), were measured with kits from SEKISUI MEDICAL (Tokyo, Japan) on an automatic biochemical analyzer from Beckman (AU5800, CA, United States). Fasting insulin (FINS) concentration was measured by enzyme-linked immunosorbent assay (ELISA) by using a kit from Millipore (EZRM1-13K, MA, United States) according to the manufacturer's instructions. Homeostasis model assessment of IR (HOMA-IR) is determined using the equations: $HOMA-IR = [FINS (mU/L) \times FPG (mmol/L)] / 22.5$.

Hematoxylin and eosin and immunohistochemistry staining for muscle sample

Muscle samples were collected and fixed in isopentane for cryopreservation at -80 °C. The muscle tissue was sliced to a thickness of 8 μm in frozen microtome by cross cutting and rip cutting. The sections were subjected to the hematoxylin and eosin (H&E) and immunohistochemical staining. For H&E staining, muscle sections of cross cutting and rip cutting were used and stained with hematoxylin for 10 min, then washed and stained with eosin for 5 min. Lastly, sections were observed under light microscope (Nikon, Japan). For immunohistochemical staining, muscle sections by cross cutting were incubated with antibody mixture of F4/80 (ab111101, Abcam, United States) and CD86 (ab213044, Abcam, United States), or F4/80 and CD206 (ab8918, Abcam, United States) at 4 °C overnight. Then slides were protected from light and incubated with secondary Alexa Fluor 488- or Alexa Fluor 555-labeled goat anti-rabbit or mouse antibodies (A-11034, A-21422, Molecular Probes, United States) for 2 h at room temperature. Counterstaining was followed with DAPI for 15 min in an aluminum foil-covered box. Finally, the stained tissues were examined under a fluorescence microscope (Leica, Germany). Six mice for each group were used, and more than eight visual fields were chosen and analyzed for each muscle section. The images were analyzed with Image Pro Plus 6.0 program (Media Cybernetics, United States). The H&E staining of cross cutting sections were used to analyze myofiber area. F4/80 positive area were used to analyze

macrophage infiltration. Co-localization of F4/80 with CD86 or CD206 were used to quantify macrophages M1 or M2 polarizations respectively.

Co-cultures RAW264.7 macrophages and C2C12 myoblasts

RAW264.7 macrophages and C2C12 myoblasts were cultured in Dulbecco's modified Eagle's Medium (DMEM; 25 mmol/L glucose; Gibco, United States) supplemented with 10% fetal bovine serum (Gibco, United States) under humidified atmosphere with 5% CO₂ at 37 °C. The 6-well and 24-well transwell co-culture system (Corning, United States) were employed for non-contactable co-culture of RAW264.7 macrophages and C2C12 myoblasts. For co-culture, 2 × 10⁶ and 4 × 10⁵ RAW264.7 macrophages were plated on upper chamber of 6-well and 24-well transwell plates, respectively. Then, 6.6 × 10⁶ and 13.3 × 10⁵ C2C12 myoblasts were plated on lower chamber of 6-well and 24-well transwell plates, respectively. Subsequently, the macrophages were plated at about 30% of the numbers of myoblasts, comparable to the abundance of macrophages observed in skeletal muscle from IR mice. The RAW264.7 macrophages and C2C12 myoblasts were allowed to adhere for 24 h before the co-culture was started. All co-culture treatments were performed for 5 d under DMEM containing 2% horse serum (Gibco, United States) to induce myogenic differentiation of myoblasts. As a control for the co-culture, the same cells were plated to the upper and lower chamber of the transwell co-culture system.

To observe the influence of HG on the interactions between myoblasts and macrophages, cells were treated with 60 mmol/L D-glucose in differentiation medium for 5 d from the start of co-culture [17,36,37]. A 60 mmol/L L-glucose was used in control group (Con group) for the HG as an osmotic control for 60 mmol/L D-glucose [38]. To detect the insulin sensitivity of myotube, C2C12 cells were incubated in the absence or presence of insulin (100 nmol/L) for 30 min at 37 °C before gathered [39,40]. After co-culture, the cells from the upper and lower chamber of the transwell system were collected separately for further biochemical and molecular analyses. Medium from these co-cultures were gathered for the assay of cytokines.

Cell viability assay

Cell viability was assessed by CCK-8 assay (APEX BIO, United States). After 5 d of treatments, 10 µL CCK-8 solution were added to RAW264.7 macrophages or C2C12 myoblasts and cultured for another 1 h. Then the absorbance was measured at a wavelength of 450 nm using Microplate Reader (Bio-Rad, Hercules, CA, United States), and the cell viability was calculated using the formula: Cell viability (%) = (A_{experimental group} - A_{blank}) / (A_{control group} - A_{blank}) × 100%. A indicates absorbance at the wavelength of 450 nm.

Morphological analysis for myotube

Cells were observed daily using light microscope to detect the effect of co-culture and HG on myoblasts morphology. After the intervention above, myotube area and number were calculated with Image Pro Plus 6.0 program (Media Cybernetics, United States). Six dishes for each group were used, and more than eight visual fields were randomly chosen and analyzed for each dish.

Flow cytometry for macrophages

After the intervention above, RAW264.7 macrophages were dissociated with trypsin-EDTA into single cell suspension. They were washed and stained with anti-CD16/32 (553142, BD Biosciences, United States) for 20 min at room temperature to block Fc receptors before incubation with PE/Cy7-labelled anti-F4/80 (ab111101, Abcam, United States), FITC-labelled anti-CD86 (ab213044, Abcam, United States), and PE-labelled anti-CD206 (ab8918, Abcam, United States) monoclonal antibodies in a dark room for 1 h. Subsequently, the cells were examined with flow cytometry (Beckman, United States). The expressions of cell markers were compared with an isotype control. The acquired flow cytometric images were analyzed with FlowJo program (version 10.0.7). The ratio of F4/80+ cells were used to quantify activated macrophage; the ratio of F4/80+CD86+CD206- cells were used to quantify M1 macrophage; the ratio of F4/80+CD206+CD86- cells were used to quantify M2 macrophage.

ELISA for culture medium

The protein levels of monocyte chemoattractant protein 1 (MCP1, MJE00B, R&D, United States, sensitivity: 0.666 pg/mL, specificity: Mouse), tumor necrosis factor-α (TNFα, MTA00B, R&D, United States, sensitivity: 7.21 pg/mL, specificity: Mouse), Interleukin-1β (IL-1β, MLB00C, R&D, United States, sensitivity: 4.8 pg/mL, specificity: Mouse), IL-6 (M6000B, R&D, United States, sensitivity: 1.8 pg/mL, specificity: Mouse), and IL-10 (M1000B, R&D, United States, sensitivity: 5.22 pg/mL, specificity: Mouse) secreted into medium was quantified with ELISA kit according to the manufacturer's instructions.

Immunohistochemistry for C2C12 myoblasts

After the intervention above, myoblasts were fixed in 4% paraformaldehyde for 15 min, and subjected to immunofluorescence staining. Myoblasts were incubated with antibody mixture of E-MHC (BF-G6, Hybridoma Bank, United States) or GLUT4 (ab654, Abcam, United States), at 4 °C overnight. Then, myoblasts were incubated with Alexa Fluor 488- or Alexa Fluor 555-labeled goat anti-rabbit or mouse antibodies (A-11034, A-21422, Molecular Probes, United States) for 2 h at room temperature. Finally, the stained cells were observed with fluorescence microscope (Leica, Germany). Six dishes for each group were used, and more than eight visual fields were randomly chosen and analyzed for each dish. The positive area of E-MHC and GLUT4 fluorescence were analyzed with Image-Pro plus 6.0 (Media Cybernetics, United States).

Glucose uptake assay for C2C12 myoblasts

After the intervention above, myotubes were starved in DMEM containing 2% fatty acid-free bovine serum albumin for 3 h, then incubated in the absence or presence of insulin (100 nM) for 30 min. Subsequently, they were incubated with 2-NBDG (Cayman, United States) (150 µg/mL) for 40 min. Fluorescence was measured using microplate reader (Bio-Rad, Hercules, CA, United States) at an excitation wavelength of 485 nm and emission wavelength of 535 nm. The negative control and blank control were set, and then standard curve generated to calculate the glucose uptake of myotube in the absence or presence of insulin, which is an indicator to evaluate the insulin sensitivity of myotube.

Statistical analysis

The data are representative of three separate experiments performed with 6 replicates. The data are reported as mean ± SD. The Shapiro-Wilk test was used to test for normality within each data set. According to the Shapiro-Wilk test, the data in each group followed a normal distribution. The two-tailed Student's *t*-test was used for comparison between two groups. The multi-group comparisons were performed with two-way ANOVA test followed by Bonferroni *post hoc* test to analyze the interaction between co-culture and HG. SPSS statistical software (version 20.0) was used for the statistical analyses, and the $P < 0.05$ was considered as statistically significant. Hedges' *g* effect sizes were calculated, and effect sizes were interpreted as: $g < 0.2$ very small, $g = 0.2-0.5$ small, $g = 0.5-0.8$ medium, $g > 0.8$ large.

RESULTS

High-fat diet fed for 12 wk induces IR in mice

Throughout the 12 wk of high-fat diet, the levels of body weight and fasting blood glucose in mice of IR group were significantly higher than Con group (Figure 1A and B; $P < 0.01$, $g > 0.8$). The levels of FINS, HOMA-IR, TG, TC, LDL-C in mice of IR group were also significantly higher than Con group (Figure 1C-E; $P < 0.01$, $g > 0.8$). To separate the response to glucose or insulin challenge from glucose homeostasis, we assessed the area under the curve of both glucose tolerance test and ITT. Glucose tolerance and insulin tolerance was impaired significantly in IR group compared with Con group (Figure 1F and G, $P < 0.01$, $g > 0.8$).

M1 macrophages increasingly infiltrated into atrophic skeletal muscle in IR mice

To detect whether IR is relevant with macrophage infiltration and M1 phenotype polarization in skeletal muscle, H&E and immunohistochemistry staining was carried on skeletal muscle. As demonstrated by H&E, skeletal muscle from IR mice displayed more inflammatory infiltration (Figure 2A, indicated with black arrows). Furthermore, by immunohistochemical staining, the positive area of F4/80 (a surface marker of macrophages) and co-localization of F4/80 and CD86 (a surface marker of M1 phenotype macrophages) was significantly increased in skeletal muscle from IR mice (Figure 2B; $P < 0.01$, $g > 0.8$). In addition, to detect the effect of IR on skeletal muscle morphology, we analyzed the cross-sectional area of myofiber. As shown in Figure 2A, myofiber size in IR group was significantly decreased than that in Con group ($P < 0.01$, $g = 6.26$).

Myoblasts in the presence of HG cooperatively induced macrophages polarizing to pro-inflammatory M1 phenotype

To understand the effect of myoblasts on macrophages polarization under HG surroundings, we researched the state of macrophages polarization in the absence or presence of myoblasts and HG. Firstly, cytotoxicity of myoblasts and HG to macrophages were tested by CCK-8 assay. As shown in Figure 3A, treatment of myoblasts and HG had no cytotoxicity on macrophages ($P > 0.05$, $g < 0.2$). By comparing the morphology of macrophages after treated without or with HG for 5 d, spindle cells and pseudopodia were observed in cells treated alone with HG (Mc + HG group) (Figure 3B, indicated with red arrows), which indicated inflammatory phenotype of macrophages in morphology. We next observed whether myoblasts also cause morphological changes of macrophages. To address this, macrophages were co-cultured with myoblasts in the presence or absence of HG. The morphology was unchanged in macrophages co-cultured with myoblasts under physiological environment (McM group), however, even more spindle cells and pseudopodia were observed in cells co-cultured with myoblasts under HG environment (McM + HG group) (Figure 3B, indicated with red arrows). Further, we examined surface markers of macrophages polarization by Flow Cytometry and expressions of related proteins in macrophages by Western Blot. Similarly, compared to Con group (Mc group), F4/80+CD86+CD206- cells were decreased and F4/80+CD206+CD86- cells were increased in McM group ($P < 0.01$, $g > 0.8$), but F4/80+CD86+CD206- cells increased and F4/80+CD206+CD86- cells were decreased in Mc + HG group ($P < 0.01$, $g > 0.8$; Figure 3C). In McM + HG group, F4/80+CD86+CD206- cells were significantly increased, and F4/80+CD206+CD86- cells were significantly decreased, compared both with Mc + HG group and McM group ($P < 0.01$, $g > 0.8$; Figure 3C).

Interactions between myoblasts and macrophages in the presence of HG concertedly increased secretion of pro-inflammatory cytokines

To verify whether the increased pro-inflammatory M1 phenotype in macrophages is complemented by increasing the secretion of cytokines, to result in chronic inflammation in muscle, we tested the protein levels of MCP1, TNF α , IL-1 β , IL-6 and IL-10 in culture medium treated as above. As shown in Figure 4, compared to Mc group, levels of pro-inflammatory TNF α , IL-1 β and IL-6 were decreased, and level of anti-inflammatory IL-10 was increased in McM group ($P < 0.01$, $g > 0.8$); but, levels of MCP1, TNF α , IL-1 β and IL-6 were increased, and level of IL-10 was decreased in Mc + HG group ($P < 0.01$, $g > 0.8$). In McM + HG group, levels of MCP1, TNF α , IL-1 β and IL-6 were significantly increased, and the expressions

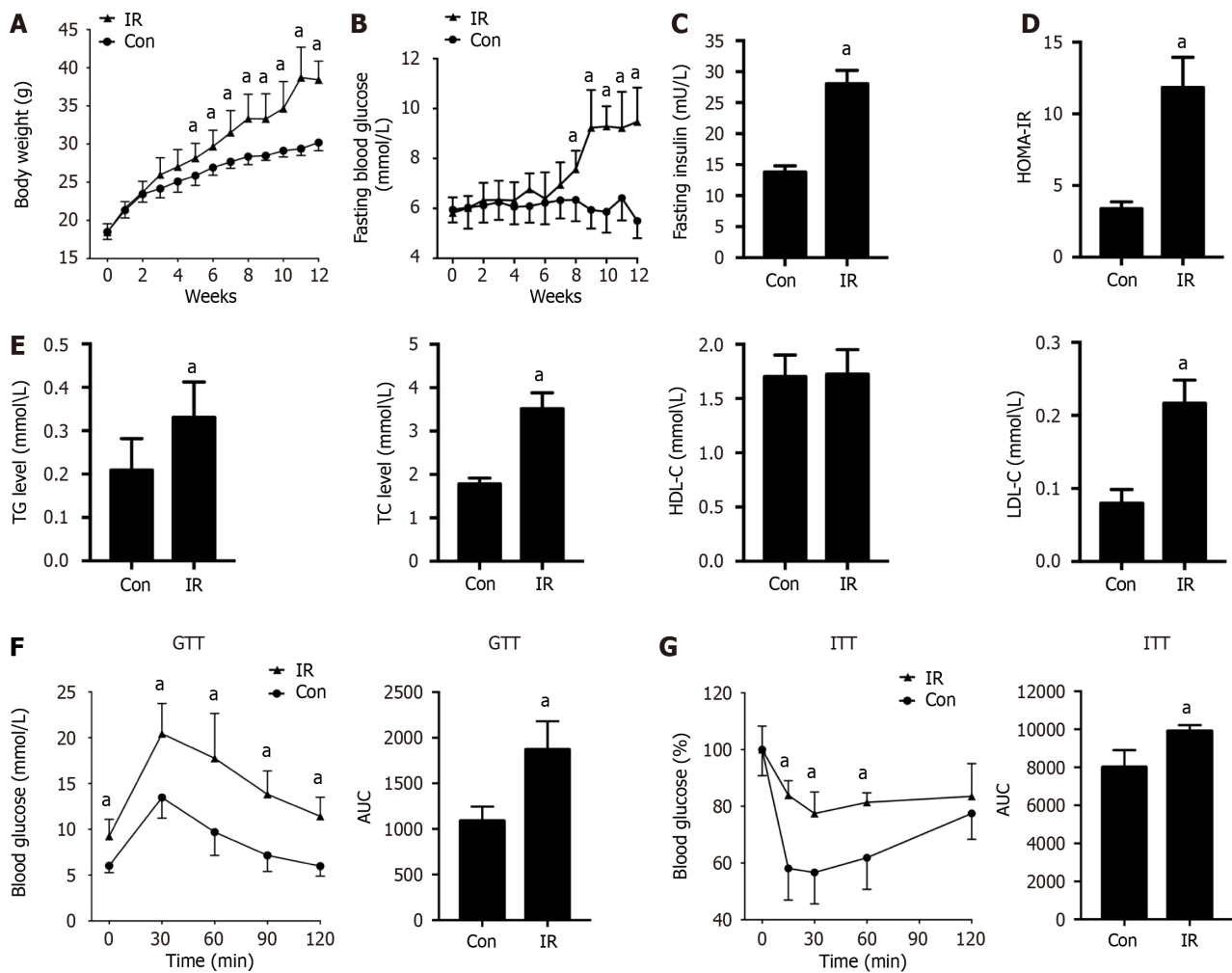


Figure 1 High-fat diet fed for 12 wk induces insulin resistance in mice. A: Body weight development of control group (Con group) and insulin resistance (IR) group mice during 12 wk fed; B: Fasting blood glucose of Con and IR group mice during 12 wk fed; C: Fasting insulin levels of Con and IR group mice fed for 12 wk; D: Homeostasis model assessment of IR of Con and IR group mice fed for 12 wk; E: Triglyceride, total cholesterol, high density lipoprotein-cholesterol, and low density lipoprotein-cholesterol concentration in serum in Con and IR group mice fed for 12 wk; F: Blood glucose values during intraperitoneal glucose tolerance tests of Con and IR group mice fed for 12 wk; G: Blood glucose values during insulin tolerance tests of Con and IR group mice fed for 12 wk. Data are means \pm SD, $n = 6$ per group. ^a $P < 0.01$ vs Con group. P values were calculated by two-tailed Student's t -test. Con: Control group; IR: Insulin resistance group; ITT: Insulin tolerance test; GTT: Glucose tolerance tests.

of IL-10 was significantly decreased, compared with both Mc + HG group and McM group ($P < 0.05$, $g > 0.8$). In brief, results showed that the state of macrophages polarization described above were also reflected in secretions of cytokines in the culture medium, which resulted in chronic inflammation environment for myoblasts.

Chronic inflammation induced by HG-related M1 macrophages efficiently inhibited myogenesis and induced myotube atrophy

To explore the mediation of HG-related M1 phenotype macrophages to myogenesis, we researched the differentiation state of myoblast in the absence or presence of macrophages and HG. Firstly, we observed the morphology of myoblasts induced for differentiation in the presence or absence of HG and macrophages for 5 d. As shown in **Figure 5A**, myoblasts in Con group (M group) differentiated into multinucleated myotube after 5 d of differentiation (indicated with red arrows), and more myotube were observed when myoblasts co-cultured with macrophages under physiological environment (MMc group, $P < 0.05$, $g > 0.8$); Whereas, area of myotube in myoblasts treated alone with HG (M + HG group) decreased compared to M group ($P < 0.01$, $g = 3.37$). Both number and area of myotube in myoblasts co-cultured with macrophages under HG environment (MMc + HG group) significantly decreased when compared with M + HG group and MMc group ($P < 0.01$, $g > 0.8$), which indicated inhibition effects of HG-related M1 phenotype macrophages on myogenesis in morphology. Then, treatments of macrophages and HG had no cytotoxicity on myoblasts by CCK-8 assay ($P > 0.05$, $g < 0.2$; **Figure 5B**). Further, we examined expression of E-MHC (marker of myotube formation) in myotube. Compared to M group, E-MHC positive area was increased in MMc group ($P < 0.01$, $g = 2.44$); but E-MHC positive area was decreased in M + HG group ($P < 0.01$, $g = 5.35$). In MMc + HG group, E-MHC positive area was significantly decreased compared both with M + HG group and MMc group ($P < 0.01$, $g = 4.19$; **Figure 5C**).

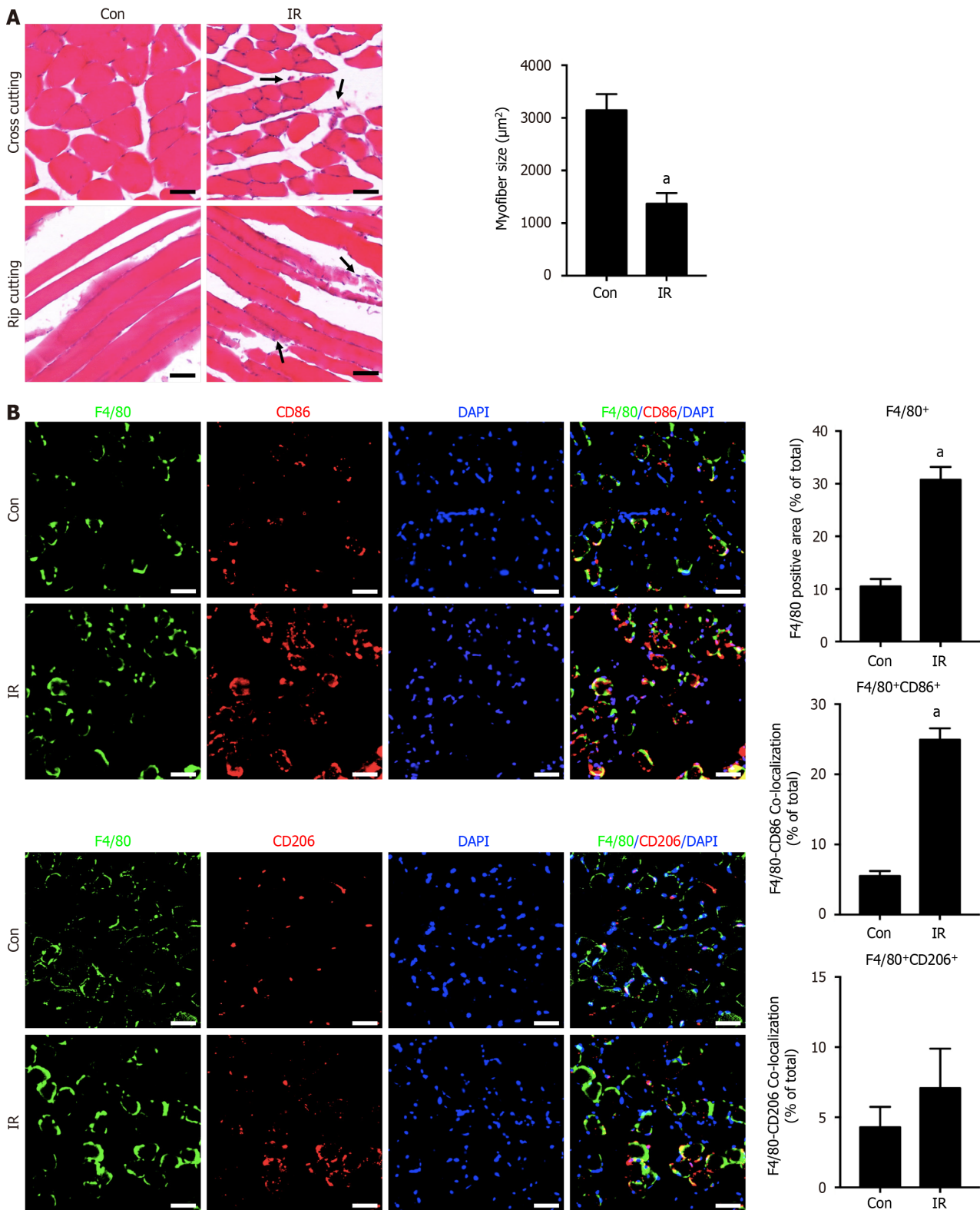


Figure 2 Insulin resistance induced myofiber atrophy and pro-inflammatory M1 phenotype macrophages infiltration in skeletal muscle. **A:** Hematoxylin eosin (H&E) staining of skeletal muscle and the areas of Myofiber (Scale bar: 50 μm); **B:** The expression of F4/80, and the co-localization of F4/80 with CD86 and CD206 respectively in skeletal muscle detected by Immunofluorescence (Scale bar: 50 μm). Data are means ± SD, *n* = 6 per group. ^a*P* < 0.01 vs Con group. *P* values were calculated by two-tailed Student's *t*-test. Con: Control group; IR: Insulin resistance group.

Chronic inflammation induced by HG-related M1 macrophages hindered insulin sensitivity in myotube

To further probe the mediation of HG-related M1 phenotype macrophages to IR in myotube, we studied the insulin action to stimulate glucose uptake and expressions of related proteins of myoblast in the absence or presence of macrophages and HG. As shown in **Figure 6**, insulin-stimulated GLUT4 fluorescence (**Figure 6A**) and glucose uptake (**Figure 6B**) were increased significantly in the M and MMC groups (*P* < 0.01, *g* > 0.8), which displayed fair insulin

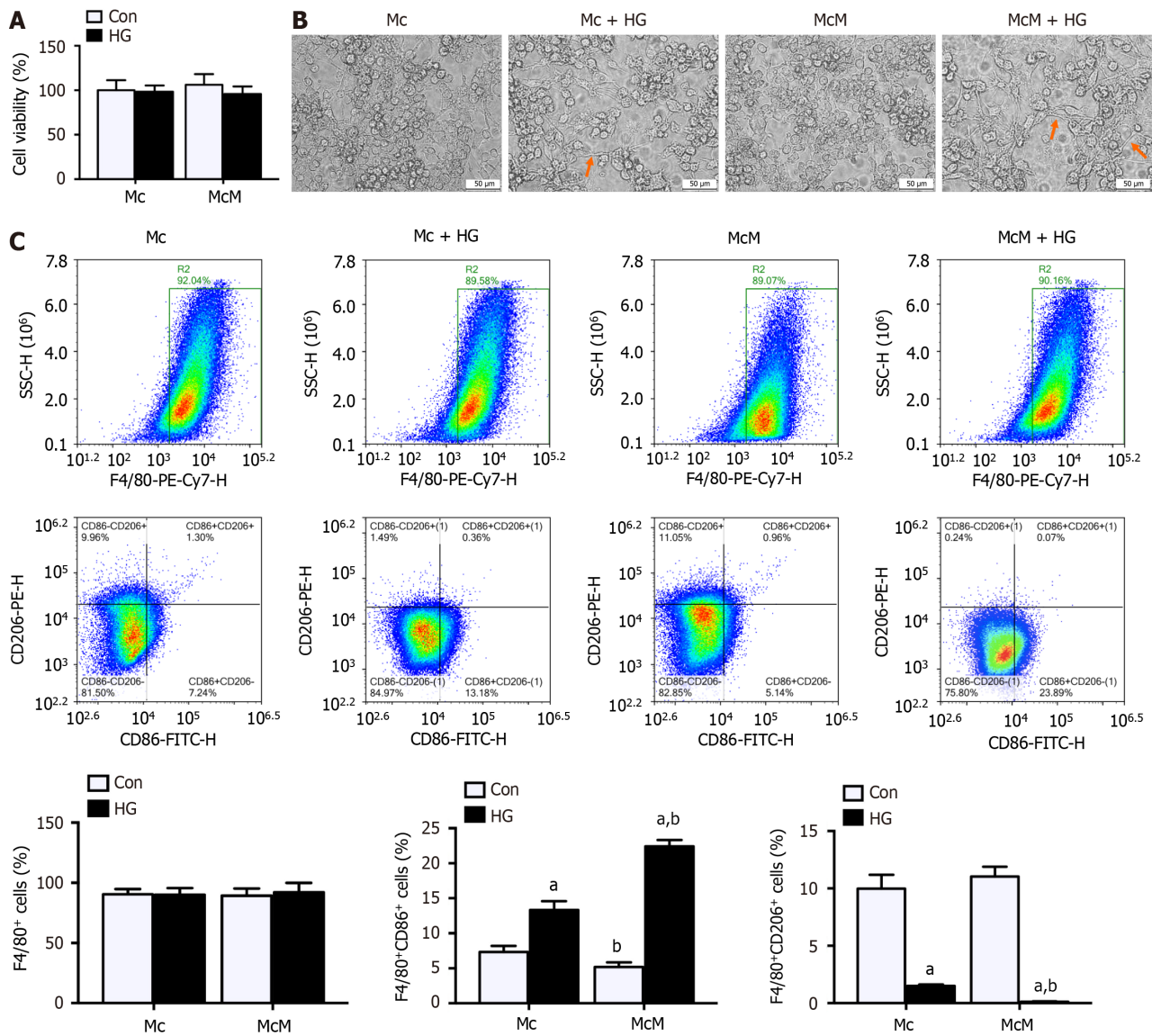


Figure 3 Myoblast under high glucose milieu resulted in macrophages polarizing to pro-inflammatory M1 phenotype. A: The viability of macrophages by CCK-8 assay; B: Representative image of macrophages by Light Microscopy, inflammatory phenotype in morphology were indicated with orange arrows (Scale bar: 50 μ m); C: The ratios of F4/80⁺ cells, F4/80⁺CD86⁺ cells, and F4/80⁺CD206⁺ cells in macrophages by Flow Cytometry. Data are means \pm SD, $n = 6$ per group. ^a $P < 0.01$ main effect of high glucose; ^b $P < 0.01$ main effect of co-cultured with myoblasts. P values were calculated by two-way analysis of variances. Mc: Macrophages; Mc + HG: Macrophages cultured in high glucose medium; McM: Macrophages co-cultured with myoblasts; McM + HG: Macrophages co-cultured with myoblasts in high glucose medium; HG: High glucose.

sensitivity of control myotube. Whereas, these insulin action in myotube were blocked by the exposure of HG (M + HG group and MMc + HG group) ($P > 0.05$, $g < 0.2$). Compared to M + HG group, both basal and the insulin-stimulated GLUT4 fluorescence and glucose uptake were decreased significantly in MMc + HG group ($P < 0.01$, $g > 0.8$).

DISCUSSION

Skeletal muscle handles about 80% of insulin-stimulated glucose uptake and become the major organ occurring IR[4,5]. HG per se result in desensitization of insulin action and induce IR, which is known as “glucose toxicity”[26-28,31]. However, despite decades of research, whether macrophages infiltration and polarization in skeletal muscle under HG milieu results in the development of IR is yet to be elucidated. Herein, the present study demonstrated the interactions between myoblasts and macrophages induce pro-inflammatory M1 polarization of macrophages to exacerbate the inflammatory state, resulting impaired myogenesis and insulin sensitivity in myoblasts under HG milieu. More concretely, we could show that: (1) Pro-Inflammatory M1 phenotype macrophages increasingly infiltrated into atrophic skeletal muscle in IR mice; (2) Myoblasts and HG cooperatively induced macrophages polarizing to pro-inflammatory M1 phenotype to aggravate inflammation; and (3) Chronic inflammation induced by HG-related M1 phenotype macrophages damage myogenesis and insulin sensitivity in myoblasts. As we have seen, this is the first report about the mediation of ma-

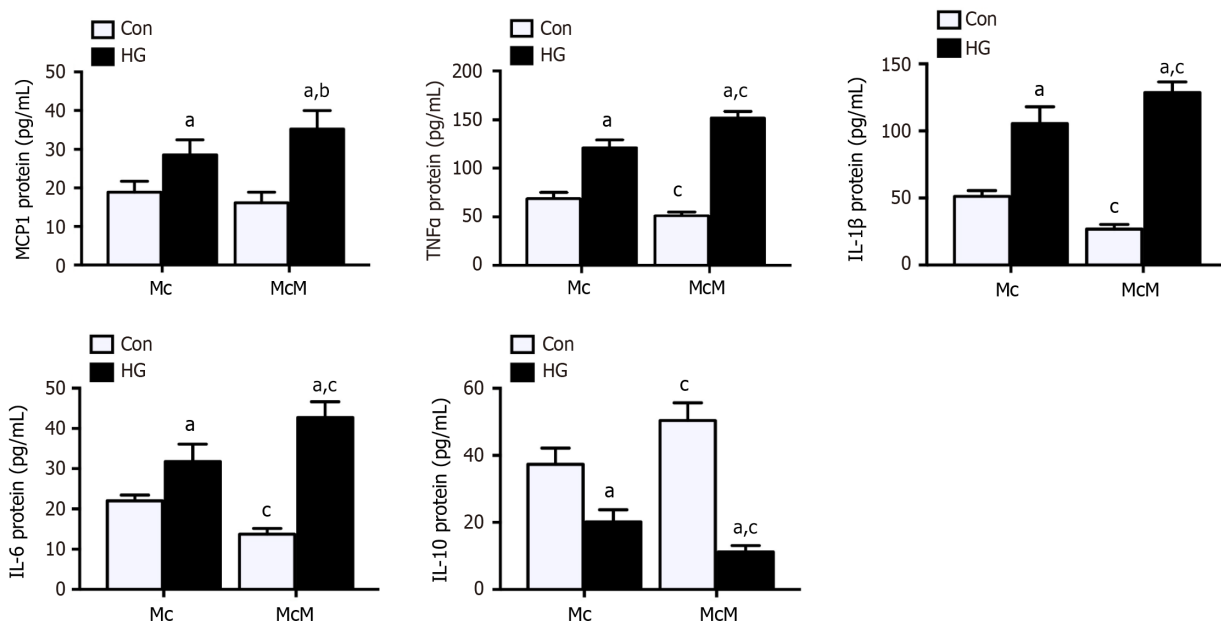


Figure 4 Interactions between myoblasts and macrophages under high glucose milieu resulted in chronic inflammation. The protein levels of monocyte chemoattractant protein 1, tumor necrosis factor- α , interleukin-1 β (IL-1 β), IL-6 and IL-10 in culture medium by enzyme-linked immunosorbent assay. Data are means \pm SD, $n = 6$ per group. ^a $P < 0.01$ main effect of high glucose; ^b $P < 0.05$, ^c $P < 0.01$ main effect of co-cultured with myoblasts. P values were calculated by two-way analysis of variances. Mc: Macrophages; Mc + HG: Macrophages cultured in high glucose medium; McM: Macrophages co-cultured with myoblasts; McM + HG: Macrophages co-cultured with myoblasts in high glucose medium; HG: High glucose.

crophages to HG-related myogenic inhibition and IR in myoblasts.

Although the pathogenesis for IR has not yet been fully elucidated, increasing evidence prove that the chronic inflammatory response in insulin-targeting tissues plays an important role in the occurrence and development of IR[13,14]. In this study, obvious inflammatory infiltration appeared in the skeletal muscle of IR mice. As predicted, our results also showed evidently smaller myofiber in IR mice, which proves the muscular atrophy in IR mice. This results are in line with some of the previous studies[41,42], which propose that the chronic inflammation contributes to skeletal muscle atrophy and sarcopenia. Currently, several studies have indicated that macrophages may mediate the occurrence of IR [17-19], but infiltration and polarization of macrophages associated with IR has not been clearly reported in skeletal muscle. Results from this study suggest that macrophages (F4/80+ cells) sharply increased in skeletal muscle of IR mice, which further polarized into classically activated pro-inflammatory macrophages (F4/80+CD86+CD206- macrophages). These findings implicated that macrophages infiltration in skeletal muscle during IR may induce seriously chronic inflammatory responses, which may result in impaired myogenesis and insulin sensitivity.

To further explore the mediation of macrophages to chronic inflammation and IR in skeletal muscle, we developed *in vitro* a co-culture system in which myoblasts were co-cultured with macrophages[17,36,37] in the exposure to HG milieu [38] to mimic the IR environment *in vivo*. Firstly, to verify the results above, we tested the activation and polarization state of macrophages in our co-culture system and correspondingly inflammatory response. Actually, the interactions between muscle and macrophages have been generous studied within the settings of skeletal injury and repair[20-23]. Some studies suggested that participation of skeletal muscle accelerates progression from an inflammatory reaction to anti-inflammatory reaction of macrophages to lastly promote myogenic differentiation and muscle repair[43]. Our results showed the presence of myoblast under physiological conditions further induced alternatively activated M2 macrophages (F4/80+CD206+CD86- cells), and then alleviated inflammation both in macrophages and surrounding environment, which is consistent with results mentioned above. However, when exposed to HG milieu, the effects of myoblasts on macrophages were completely reversed. HG milieu induced macrophages abundantly polarized into classically activated M1 macrophages, and then aggravated chronic inflammation both in macrophages and surrounding environment. What's more, compared to expose to HG milieu alone, macrophages more tend to polarize to pro-inflammatory M1 phenotype under the cooperations of HG milieu with myoblasts. These results testified the co-culture system in this study in the presence of HG milieu is capable of inducing classically activated pro-inflammatory macrophages, which is compatible with the findings *in vivo*.

Although macrophages infiltration associated with IR has not been clearly reported in skeletal muscle, many studies have confirmed the interactions between skeletal muscle and macrophages regulated the inflammatory reaction and regeneration in skeletal muscle[20,21]. Our results again confirmed the fact that macrophages are capable of promoting myogenesis in physiological environment, which have proposed in several recent studies[44,45]. However, when exposed to HG milieu, the effects of macrophages to promote myogenesis were reversed. Myogenic differentiation is crucial for muscle repair and quality maintenance, which were obviously suppressed in HG milieu. What's more, the participation of macrophages in HG environment led to more seriously myogenic inhibition. These results suggested inflammatory reaction induced by HG-related pro-inflammatory macrophages efficiently inhibited myogenesis and induced myotube

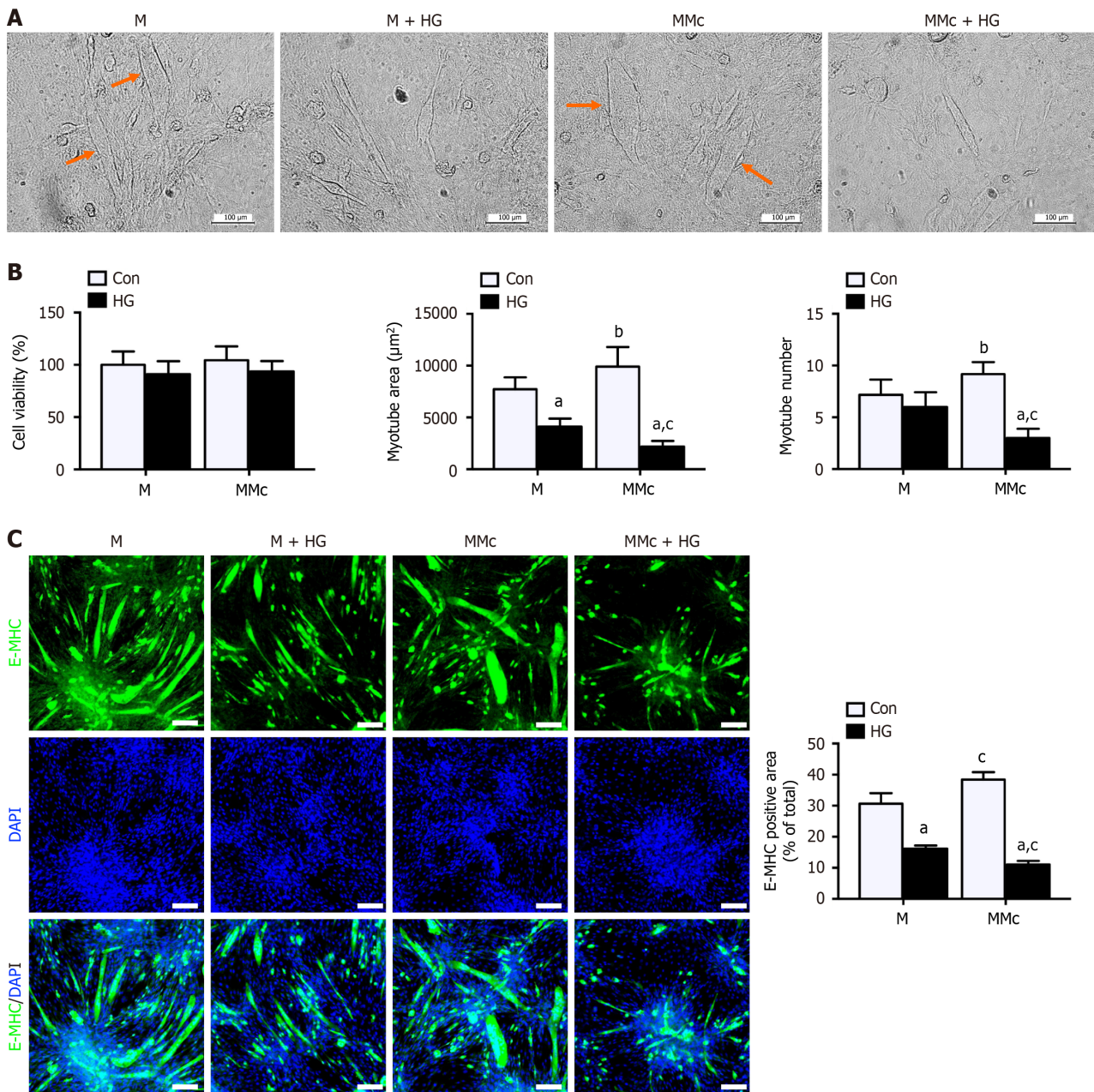


Figure 5 Inflammatory reaction induced by M1 macrophages inhibited myogenic differentiation and led to myotube atrophy. A: Representative image of myotube by light microscopy, myotube were indicated with orange arrows (scale bar: 100 µm); B: The viability of myoblasts by CCK-8 assay; C: The ratios of E-MHC positive area in myotube by Immunofluorescence (scale bar: 50 µm). Data are means ± SD, n = 6 per group. ^aP < 0.05, ^bP < 0.01 main effect of high glucose; ^cP < 0.01 main effect of co-cultured with macrophages. P values were calculated by two-way analysis of variances. M: Myoblasts; M + HG: Myoblasts cultured in high glucose medium; MMc: Myoblasts co-cultured with macrophages; MMc + HG: Myoblasts co-cultured with macrophages in high glucose medium; HG: High glucose.

atrophy.

Numerous researches have demonstrated the vicious cycle between myoatrophy and IR[7,8], which prompts myogenic inhibition induced by HG-related classically activated pro-inflammatory macrophages may further hinder insulin sensitivity in myotube. The GLUT4 translocation is indispensable for glucose transport in skeletal muscle and myoblast, and also participated in adjusting to myogenesis[46,47]. In this research, the actions of insulin to stimulate GLUT4 translocation and glucose uptake in myotube were augmented in the presence of macrophages in physiological environment, which suggested increased insulin sensitivity of myotube. Whereas, when exposed to HG milieu, the effects of macrophages to increase insulin sensitivity in myotube were reversed. Both basal and insulin-stimulated GLUT4 translocation and glucose uptake down-regulated in HG milieu. Further, consistently with the effect on myogenic differentiation, the participation of macrophages in HG environment led to more serious IR. These results suggested inflammatory reaction induced by HG-related classically activated pro-inflammatory macrophages efficiently hindered insulin sensitivity in myotube.

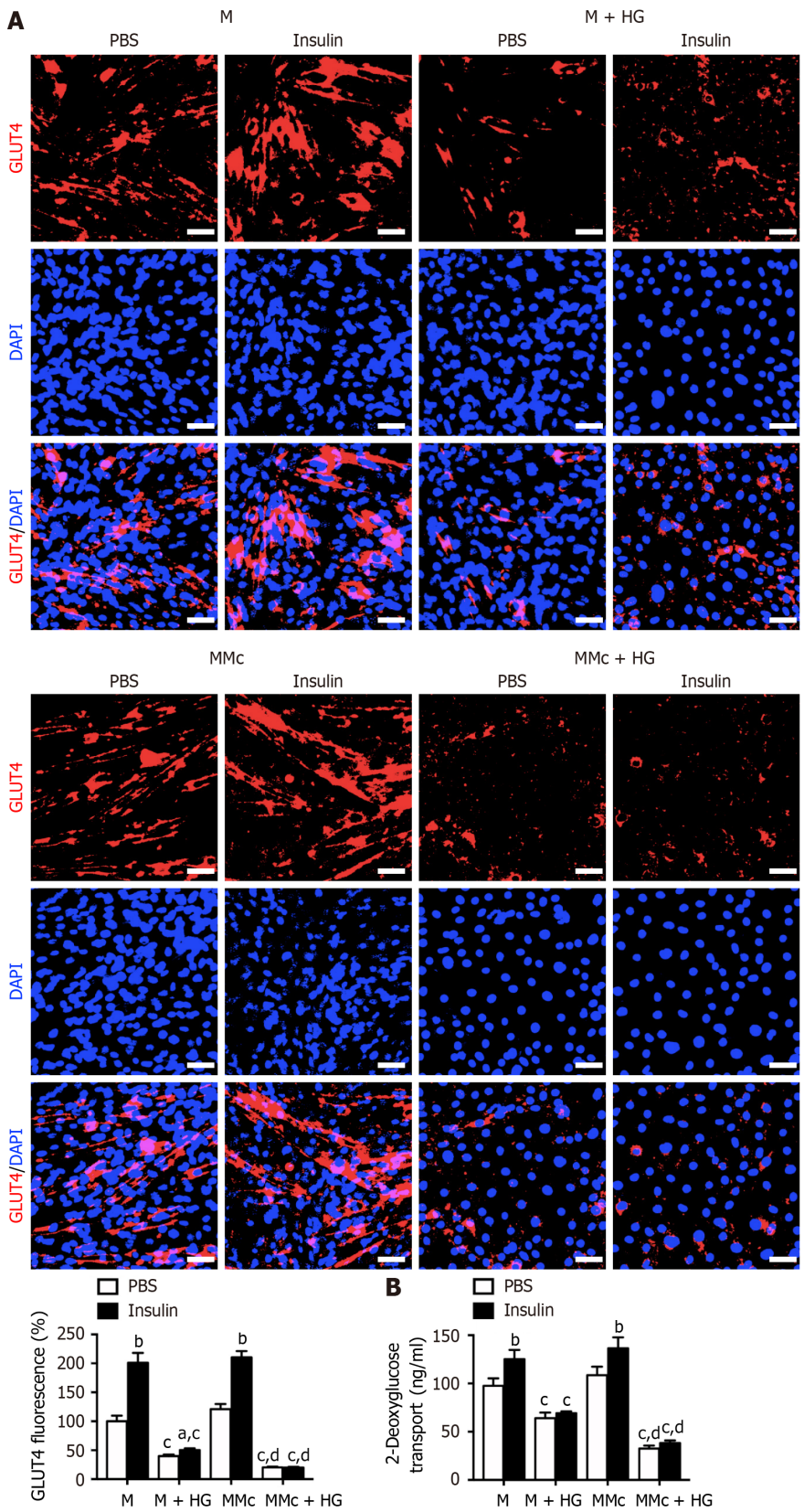


Figure 6 Inflammatory reaction induced by M1 macrophages impaired myotube insulin sensitivity. A: The GLUT4 fluorescence of myotube in the absence or presence of 100 nmo/L insulin by Immunofluorescence (scale bar: 50 μm); B: The 2-Deoxyglucose transport of myotube in the absence or presence of 100 nmo/L insulin by glucose uptake assay. Data are means ± SD, n = 6 per group. ^aP < 0.05, ^bP < 0.01 main effect of insulin; ^cP < 0.01 main effect of high glucose; ^dP < 0.01 main effect of co-cultured with macrophages. P values were calculated by two-way analysis of variances. M: Myoblasts; M + HG: Myoblasts cultured in high glucose medium; MMc: Myoblasts co-cultured with macrophages; MMc + HG: Myoblasts co-cultured with macrophages in high glucose medium; HG: High glucose.

In addition, 25 mmol/L glucose is recommended by the American Type Culture Collection for myoblasts culture, so DMEM with 25 mmol/L glucose should be regarded as the norm caloric conditions[48]. For the HG milieu, we originally treated macrophages and myoblasts with 40 mmol/L or 60 mmol/L glucose. By preliminary experiments, we found that 40 mmol/L glucose had a slight but non-significant effect on macrophages polarization and myoblasts differentiation, but 60 mmol/L glucose significantly induced M1 macrophages and inhibited myoblasts differentiation. Since the main aim of this study is to explore the potential mechanisms of HG inducing inflammatory response and myoblasts IR, the glucose dosage that significantly effected macrophages polarization and myoblasts differentiation should be used. So, in this study, we used 60 mmol/L glucose as the HG condition. However, this study has certain limitations. Firstly, in order to really demonstrate the effects on inflammation and IR in this study are just related to glucose per se and not to hyperosmolarity induced by 60 mmol/L glucose, we used L-glucose as an osmotic control for 60 mmol/L D-glucose. So, future research may be needed to analyze the damage of hyperosmolarity caused by HG to inflammation and insulin sensitivity. Further, the sample size ($n = 6$ per group) may be relatively small in this study, the study with higher sample size would be needed to reconfirm the results of this study.

In summary, the current study revealed that macrophages promoted myogenesis in physiological conditions, but interactions between myoblasts and macrophages under HG milieu induced pro-inflammatory M1 polarization of macrophages to exacerbate inflammatory response. Subsequently, chronic inflammation induced by HG-related M1 macrophages damaged myogenesis and insulin sensitivity in myoblasts, which ultimately resulted in skeletal muscle IR. This is the first research about the mediation of macrophages to HG-related myogenic inhibition and IR in myoblasts, which supported macrophage may serve as a promising therapeutic target for skeletal muscle atrophy and IR. This study provides new insights into the prevention and treatment of skeletal muscle atrophy and IR, which may contribute to further explore *in vivo* the pathogeny of IR and the involvement of macrophages.

CONCLUSION

Overall, interactions between myoblasts and macrophages under HG milieu induced pro-inflammatory M1 polarization of macrophages to exacerbate inflammatory response, which ultimately resulted in skeletal muscle atrophy and IR. These findings provide new insights into the prevention and treatment of skeletal muscle atrophy and IR, which support macrophage may serve as a promising therapeutic target for skeletal muscle atrophy and IR.

FOOTNOTES

Author contributions: Ai L, Luo W and Zhou Y designed the research study; Luo W, Zhou Y, Wang LY and Ai L performed the research; Luo W, Ai L and Wang LY analyzed the data and wrote the manuscript; All authors have read and approve the final manuscript.

Supported by National Natural Science Foundation of China, No. 32200944; “Qing Lan” Project of Jiangsu Province; and the Jiangsu Research Institute of Sports Science Foundation, No. BM-2023-03.

Institutional animal care and use committee statement: All procedures involving animals were reviewed and approved by the Institutional Animal Care and Use Committee of Nanjing Sport Institute (Protocol No. GZRDW-2022-02).

Conflict-of-interest statement: All the authors report no relevant conflicts of interest for this article.

Data sharing statement: The data are available on reasonable request at ailei_982@163.com.

ARRIVE guidelines statement: The authors have read the ARRIVE Guidelines, and the manuscript was prepared and revised according to the ARRIVE Guidelines.

Open-Access: This article is an open-access article that was selected by an in-house editor and fully peer-reviewed by external reviewers. It is distributed in accordance with the Creative Commons Attribution NonCommercial (CC BY-NC 4.0) license, which permits others to distribute, remix, adapt, build upon this work non-commercially, and license their derivative works on different terms, provided the original work is properly cited and the use is non-commercial. See: <https://creativecommons.org/licenses/by-nc/4.0/>

Country of origin: China

ORCID number: Lei Ai [0000-0002-8406-3900](https://orcid.org/0000-0002-8406-3900).

S-Editor: Li L

L-Editor: A

P-Editor: Zhao S

REFERENCES

- 1 Liu FP, Guo MJ, Yang Q, Li YY, Wang YG, Zhang M. Myosteatorosis is associated with coronary artery calcification in patients with type 2 diabetes. *World J Diabetes* 2024; **15**: 429-439 [PMID: 38591084 DOI: 10.4239/wjcd.v15.i3.429]
- 2 Ortiz GG, Huerta M, González-Usigli HA, Torres-Sánchez ED, Delgado-Lara DL, Pacheco-Moisés FP, Mireles-Ramírez MA, Torres-Mendoza BM, Moreno-Cih RI, Velázquez-Brizuela IE. Cognitive disorder and dementia in type 2 diabetes mellitus. *World J Diabetes* 2022; **13**: 319-337 [PMID: 35582669 DOI: 10.4239/wjcd.v13.i4.319]
- 3 Russo B, Picconi F, Malandrucchio I, Frontoni S. Flavonoids and Insulin-Resistance: From Molecular Evidences to Clinical Trials. *Int J Mol Sci* 2019; **20** [PMID: 31027340 DOI: 10.3390/ijms20092061]
- 4 Neves KB, Nguyen Dinh Cat A, Alves-Lopes R, Harvey KY, Costa RMD, Lobato NS, Montezano AC, Oliveira AM, Touyz RM, Tostes RC. Chemerin receptor blockade improves vascular function in diabetic obese mice *via* redox-sensitive and Akt-dependent pathways. *Am J Physiol Heart Circ Physiol* 2018; **315**: H1851-H1860 [PMID: 30216119 DOI: 10.1152/ajpheart.00285.2018]
- 5 Fujimoto BA, Young M, Carter L, Pang APS, Corley MJ, Fogelgren B, Polgar N. The exocyst complex regulates insulin-stimulated glucose uptake of skeletal muscle cells. *Am J Physiol Endocrinol Metab* 2019; **317**: E957-E972 [PMID: 31593505 DOI: 10.1152/ajpendo.00109.2019]
- 6 Turner MC, Player DJ, Martin NRW, Akam EC, Lewis MP. The effect of chronic high insulin exposure upon metabolic and myogenic markers in C2C12 skeletal muscle cells and myotubes. *J Cell Biochem* 2018; **119**: 5686-5695 [PMID: 29384221 DOI: 10.1002/jcb.26748]
- 7 Rubio-Ruiz ME, Guarner-Lans V, Pérez-Torres I, Soto ME. Mechanisms Underlying Metabolic Syndrome-Related Sarcopenia and Possible Therapeutic Measures. *Int J Mol Sci* 2019; **20** [PMID: 30717377 DOI: 10.3390/ijms20030647]
- 8 Consitt LA, Clark BC. The Vicious Cycle of Myostatin Signaling in Sarcopenic Obesity: Myostatin Role in Skeletal Muscle Growth, Insulin Signaling and Implications for Clinical Trials. *J Frailty Aging* 2018; **7**: 21-27 [PMID: 29412438 DOI: 10.14283/jfa.2017.33]
- 9 Dirks ML, Wall BT, van de Valk B, Holloway TM, Holloway GP, Chabowski A, Goossens GH, van Loon LJ. One Week of Bed Rest Leads to Substantial Muscle Atrophy and Induces Whole-Body Insulin Resistance in the Absence of Skeletal Muscle Lipid Accumulation. *Diabetes* 2016; **65**: 2862-2875 [PMID: 27358494 DOI: 10.2337/db15-1661]
- 10 Akscyn RM, Franklin JL, Gavrikova TA, Messina JL. Skeletal muscle atrogene expression and insulin resistance in a rat model of polytrauma. *Physiol Rep* 2016; **4** [PMID: 26818585 DOI: 10.14814/phy2.12659]
- 11 Sampath Kumar A, Maiya AG, Shastry BA, Vaishali K, Ravishankar N, Hazari A, Gundmi S, Jadhav R. Exercise and insulin resistance in type 2 diabetes mellitus: A systematic review and meta-analysis. *Ann Phys Rehabil Med* 2019; **62**: 98-103 [PMID: 30553010 DOI: 10.1016/j.rehab.2018.11.001]
- 12 Ha MS, Son WM. Combined exercise is a modality for improving insulin resistance and aging-related hormone biomarkers in elderly Korean women. *Exp Gerontol* 2018; **114**: 13-18 [PMID: 30359693 DOI: 10.1016/j.exger.2018.10.012]
- 13 Wu H, Ballantyne CM. Skeletal muscle inflammation and insulin resistance in obesity. *J Clin Invest* 2017; **127**: 43-54 [PMID: 28045398 DOI: 10.1172/JCI88880]
- 14 Xiong XQ, Geng Z, Zhou B, Zhang F, Han Y, Zhou YB, Wang JJ, Gao XY, Chen Q, Li YH, Kang YM, Zhu GQ. FNDC5 attenuates adipose tissue inflammation and insulin resistance *via* AMPK-mediated macrophage polarization in obesity. *Metabolism* 2018; **83**: 31-41 [PMID: 29374559 DOI: 10.1016/j.metabol.2018.01.013]
- 15 Hamidzadeh K, Christensen SM, Dalby E, Chandrasekaran P, Mosser DM. Macrophages and the Recovery from Acute and Chronic Inflammation. *Annu Rev Physiol* 2017; **79**: 567-592 [PMID: 27959619 DOI: 10.1146/annurev-physiol-022516-034348]
- 16 Oishi Y, Manabe I. Macrophages in inflammation, repair and regeneration. *Int Immunol* 2018; **30**: 511-528 [PMID: 30165385 DOI: 10.1093/intimm/dxy054]
- 17 Varma V, Yao-Borengasser A, Rasouli N, Nolen GT, Phanavanh B, Starks T, Gurley C, Simpson P, McGehee RE Jr, Kern PA, Peterson CA. Muscle inflammatory response and insulin resistance: synergistic interaction between macrophages and fatty acids leads to impaired insulin action. *Am J Physiol Endocrinol Metab* 2009; **296**: E1300-E1310 [PMID: 19336660 DOI: 10.1152/ajpendo.90885.2008]
- 18 Russo L, Lumeng CN. Properties and functions of adipose tissue macrophages in obesity. *Immunology* 2018; **155**: 407-417 [PMID: 30229891 DOI: 10.1111/imm.13002]
- 19 Lee Y, Ka SO, Cha HN, Chae YN, Kim MK, Park SY, Bae EJ, Park BH. Myeloid Sirtuin 6 Deficiency Causes Insulin Resistance in High-Fat Diet-Fed Mice by Eliciting Macrophage Polarization Toward an M1 Phenotype. *Diabetes* 2017; **66**: 2659-2668 [PMID: 28607107 DOI: 10.2337/db16-1446]
- 20 Yin Y, Hao H, Cheng Y, Zang L, Liu J, Gao J, Xue J, Xie Z, Zhang Q, Han W, Mu Y. Human umbilical cord-derived mesenchymal stem cells direct macrophage polarization to alleviate pancreatic islets dysfunction in type 2 diabetic mice. *Cell Death Dis* 2018; **9**: 760 [PMID: 29988034 DOI: 10.1038/s41419-018-0801-9]
- 21 Latroche C, Weiss-Gayet M, Muller L, Gitiaux C, Leblanc P, Liot S, Ben-Larbi S, Abou-Khalil R, Verger N, Bardot P, Magnan M, Chrétien F, Mounier R, Germain S, Chazaud B. Coupling between Myogenesis and Angiogenesis during Skeletal Muscle Regeneration Is Stimulated by Restorative Macrophages. *Stem Cell Reports* 2017; **9**: 2018-2033 [PMID: 29198825 DOI: 10.1016/j.stemcr.2017.10.027]
- 22 Farup J, Madaro L, Puri PL, Mikkelsen UR. Interactions between muscle stem cells, mesenchymal-derived cells and immune cells in muscle homeostasis, regeneration and disease. *Cell Death Dis* 2015; **6**: e1830 [PMID: 26203859 DOI: 10.1038/cddis.2015.198]
- 23 Dort J, Fabre P, Molina T, Dumont NA. Macrophages Are Key Regulators of Stem Cells during Skeletal Muscle Regeneration and Diseases. *Stem Cells Int* 2019; **2019**: 4761427 [PMID: 31396285 DOI: 10.1155/2019/4761427]
- 24 Ceafalan LC, Fertig TE, Popescu AC, Popescu BO, Hinescu ME, Gherghiceanu M. Skeletal muscle regeneration involves macrophage-myoblast bonding. *Cell Adh Migr* 2018; **12**: 228-235 [PMID: 28759306 DOI: 10.1080/19336918.2017.1346774]
- 25 Luo W, Ai L, Wang B, Wang L, Gan Y, Liu C, Jensen J, Zhou Y. Eccentric exercise and dietary restriction inhibits M1 macrophage polarization activated by high-fat diet-induced obesity. *Life Sci* 2020; **243**: 117246 [PMID: 31904367 DOI: 10.1016/j.lfs.2019.117246]
- 26 Zhang HH, Ma XJ, Wu LN, Zhao YY, Zhang PY, Zhang YH, Shao MW, Liu F, Li F, Qin GJ. SIRT1 attenuates high glucose-induced insulin resistance *via* reducing mitochondrial dysfunction in skeletal muscle cells. *Exp Biol Med (Maywood)* 2015; **240**: 557-565 [PMID: 25710929 DOI: 10.1177/1535370214557218]
- 27 Zhan X, Yan C, Chen Y, Wei X, Xiao J, Deng L, Yang Y, Qiu P, Chen Q. Celastrol antagonizes high glucose-evoked podocyte injury, inflammation and insulin resistance by restoring the HO-1-mediated autophagy pathway. *Mol Immunol* 2018; **104**: 61-68 [PMID: 30439604 DOI: 10.1016/j.molimm.2018.10.021]
- 28 Johnson HM, Stanfield E, Campbell GJ, Eberl EE, Cooney GJ, Bell-Anderson KS. Glucose mediates insulin sensitivity *via* a hepatportal

- mechanism in high-fat-fed rats. *J Endocrinol* 2019; **241**: 189-199 [PMID: 30939450 DOI: 10.1530/JOE-18-0566]
- 29 **Hansen D**, De Strijcker D, Calders P. Impact of Endurance Exercise Training in the Fasted State on Muscle Biochemistry and Metabolism in Healthy Subjects: Can These Effects be of Particular Clinical Benefit to Type 2 Diabetes Mellitus and Insulin-Resistant Patients? *Sports Med* 2017; **47**: 415-428 [PMID: 27459862 DOI: 10.1007/s40279-016-0594-x]
- 30 **Ying W**, Riopel M, Bandyopadhyay G, Dong Y, Birmingham A, Seo JB, Ofrecio JM, Wollam J, Hernandez-Carretero A, Fu W, Li P, Olefsky JM. Adipose Tissue Macrophage-Derived Exosomal miRNAs Can Modulate In Vivo and In Vitro Insulin Sensitivity. *Cell* 2017; **171**: 372-384.e12 [PMID: 28942920 DOI: 10.1016/j.cell.2017.08.035]
- 31 **Zhang W**, Wu M, Kim T, Jariwala RH, Garvey WJ, Luo N, Kang M, Ma E, Tian L, Steverson D, Yang Q, Fu Y, Garvey WT. Skeletal Muscle TRIB3 Mediates Glucose Toxicity in Diabetes and High-Fat Diet-Induced Insulin Resistance. *Diabetes* 2016; **65**: 2380-2391 [PMID: 27207527 DOI: 10.2337/db16-0154]
- 32 **Mohan R**, Jo S, Lockridge A, Ferrington DA, Murray K, Eschenlauer A, Bernal-Mizrachi E, Fujitani Y, Alejandro EU. OGT Regulates Mitochondrial Biogenesis and Function via Diabetes Susceptibility Gene Pdx1. *Diabetes* 2021; **70**: 2608-2625 [PMID: 34462257 DOI: 10.2337/db21-0468]
- 33 **Raposo HF**, Vanzela EC, Berti JA, Oliveira HC. Cholesteryl Ester Transfer Protein (CETP) expression does not affect glucose homeostasis and insulin secretion: studies in human CETP transgenic mice. *Lipids Health Dis* 2016; **15**: 9 [PMID: 26758205 DOI: 10.1186/s12944-016-0179-6]
- 34 **Roduit R**, Masiello P, Wang SP, Li H, Mitchell GA, Prentki M. A role for hormone-sensitive lipase in glucose-stimulated insulin secretion: a study in hormone-sensitive lipase-deficient mice. *Diabetes* 2001; **50**: 1970-1975 [PMID: 11522661 DOI: 10.2337/diabetes.50.9.1970]
- 35 **Abdollahi A**, Dowden BN, Buhman KK, Zembroski AS, Henderson GC. Albumin knockout mice exhibit reduced plasma free fatty acid concentration and enhanced insulin sensitivity. *Physiol Rep* 2022; **10**: e15161 [PMID: 35238481 DOI: 10.14814/phy2.15161]
- 36 **Kravchenko IV**, Furaletv VA, Popov VO. The Influence of Myofibrils on the Proliferation and Differentiation of Myoblasts Cocultured with Macrophages. *Dokl Biochem Biophys* 2018; **479**: 72-76 [PMID: 29779100 DOI: 10.1134/S1607672918020060]
- 37 **Talari M**, Kapadia B, Kain V, Seshadri S, Prajapati B, Rajput P, Misra P, Parsa KV. MicroRNA-16 modulates macrophage polarization leading to improved insulin sensitivity in myoblasts. *Biochimie* 2015; **119**: 16-26 [PMID: 26453808 DOI: 10.1016/j.biochi.2015.10.004]
- 38 **Luo W**, Ai L, Wang BF, Zhou Y. High glucose inhibits myogenesis and induces insulin resistance by down-regulating AKT signaling. *Biomed Pharmacother* 2019; **120**: 109498 [PMID: 31634780 DOI: 10.1016/j.biopha.2019.109498]
- 39 **Grzelkowska-Kowalczyk K**, Wieteska-Skrzeczynska W. Treatment with IFN-gamma prevents insulin-dependent PKB, p70S6k phosphorylation and protein synthesis in mouse C2C12 myogenic cells. *Cell Biol Int* 2009; **34**: 117-124 [PMID: 19947939 DOI: 10.1042/CBI20090135]
- 40 **Kellerer M**, Koch M, Metzinger E, Mushack J, Capp E, Häring HU. Leptin activates PI-3 kinase in C2C12 myotubes via janus kinase-2 (JAK-2) and insulin receptor substrate-2 (IRS-2) dependent pathways. *Diabetologia* 1997; **40**: 1358-1362 [PMID: 9389430 DOI: 10.1007/s001250050832]
- 41 **Bitar MS**, Nader J, Al-Ali W, Al Madhoun A, Arefanian H, Al-Mulla F. Hydrogen Sulfide Donor NaHS Improves Metabolism and Reduces Muscle Atrophy in Type 2 Diabetes: Implication for Understanding Sarcopenic Pathophysiology. *Oxid Med Cell Longev* 2018; **2018**: 6825452 [PMID: 30510624 DOI: 10.1155/2018/6825452]
- 42 **Gatineau E**, Savary-Auzeloux I, Migné C, Polakof S, Dardevet D, Mosoni L. Chronic Intake of Sucrose Accelerates Sarcopenia in Older Male Rats through Alterations in Insulin Sensitivity and Muscle Protein Synthesis. *J Nutr* 2015; **145**: 923-930 [PMID: 25809681 DOI: 10.3945/jn.114.205583]
- 43 **Chazaud B**. Inflammation during skeletal muscle regeneration and tissue remodeling: application to exercise-induced muscle damage management. *Immunol Cell Biol* 2016; **94**: 140-145 [PMID: 26526620 DOI: 10.1038/icb.2015.97]
- 44 **Wehling-Henricks M**, Welc SS, Samengo G, Rinaldi C, Lindsey C, Wang Y, Lee J, Kuro-O M, Tidball JG. Macrophages escape Klotho gene silencing in the mdx mouse model of Duchenne muscular dystrophy and promote muscle growth and increase satellite cell numbers through a Klotho-mediated pathway. *Hum Mol Genet* 2018; **27**: 14-29 [PMID: 29040534 DOI: 10.1093/hmg/ddx380]
- 45 **Ogle ME**, Segar CE, Sridhar S, Botchwey EA. Monocytes and macrophages in tissue repair: Implications for immunoregenerative biomaterial design. *Exp Biol Med (Maywood)* 2016; **241**: 1084-1097 [PMID: 27229903 DOI: 10.1177/1535370216650293]
- 46 **Sharma BR**, Kim HJ, Rhyu DY. Caulerpa lentillifera extract ameliorates insulin resistance and regulates glucose metabolism in C57BL/KsJ-db/db mice via PI3K/AKT signaling pathway in myocytes. *J Transl Med* 2015; **13**: 62 [PMID: 25889508 DOI: 10.1186/s12967-015-0412-5]
- 47 **Vlavcheski F**, Baron D, Vlachogiannis IA, MacPherson REK, Tsiani E. Carnosol Increases Skeletal Muscle Cell Glucose Uptake via AMPK-Dependent GLUT4 Glucose Transporter Translocation. *Int J Mol Sci* 2018; **19** [PMID: 29710819 DOI: 10.3390/ijms19051321]
- 48 **Khilji S**, Hamed M, Chen J, Li Q. Loci-specific histone acetylation profiles associated with transcriptional coactivator p300 during early myoblast differentiation. *Epigenetics* 2018; **13**: 642-654 [PMID: 29927685 DOI: 10.1080/15592294.2018.1489659]



Published by **Baishideng Publishing Group Inc**
7041 Koll Center Parkway, Suite 160, Pleasanton, CA 94566, USA
Telephone: +1-925-3991568
E-mail: office@baishideng.com
Help Desk: <https://www.f6publishing.com/helpdesk>
<https://www.wjgnet.com>

